PAPER

Check for updates

Dynamic response study of Ti₃C₂-MXene films to shockwave and impact forces†

Shreyas Srivatsa, [ID] *[a] Pavithra Belthangadi,[b] Shivakarthik Ekambaram,[c] Manu Pai,[d] Prosenjit Sen,[b] Tadeusz Uhl, [ID] [a] Saurabh Kumar, [ID] *[b] Krzysztof Grabowski [ID] *[a] and M. M. Nayak[b]

MXenes (Titanium Carbide, Ti₃C₂-MXene) are two-dimensional nanomaterials that are known for their conductivity, film-forming ability, and elasticity. Though literature reports the possibility of usage of Ti₃C₂-MXenes for sensor development, the material properties and response need be studied in detail for designing sensors to measure dynamic variables like force, displacement, *etc.*, in a dynamic environment. Ti₃C₂-MXenes due to their good electro-mechanical properties can be used for manufacturing sensing elements for engineering and biomedical applications. This paper focuses on an investigation of the dynamic response properties of Ti₃C₂-MXenes subjected to shockwave and impact forces. A supersonic shockwave (Mach number: 1.68, peak overpressure: 234.3 kPa) produced in a shock tube acts as an external force on the Ti₃C₂-MXene film placed inside the shock tube. In the experiment performed, the response time of the Ti₃C₂-MXene film sample has been observed to be in the range of few microseconds (∼7 μs) for the high-velocity shock. In a separate experiment, Ti₃C₂-MXene film samples are subjected to low-velocity impact forces through a ball drop test. The results from the ball drop test provide a response time in the range of few milliseconds (average ∼1.5 ms). In this novel demonstration, the Ti₃C₂-MXene film sample responds well for both low-velocity mechanical impact as well as high-velocity shockwave impact. Further, the repeatability of the dynamic response of the Ti₃C₂-MXene film sample is discussed along with its significant piezoresistive behavior. This work provides the basis for sensor development to measure the dynamic phenomena of pressure changes, acoustic emissions, structural vibrations, *etc.*

Introduction

Measurement of dynamic phenomena in engineering systems including mechanical, aerospace structures *etc.*, and in biomedical devices is very important from the system control and health monitoring point of view. These measurements require dedicated sensors with properties that do not affect the measured quantity. Common sensor design includes sensing elements, signal conditioning electronics, power supply, input/output connectors, packaging, *etc.* In the design of sensors for dynamic measurements, one of the most important factors is

the right choice of sensing element material. The dynamic response parameters (*e.g.* response time) of the sensing element material need to fit well for the requirements of sensor design for various dynamic loading conditions. The sensing element may transform field variables (displacement, strains, temperature, force, *etc.*) of the structure into electrical signals that can be further processed by microcontroller or other computing devices. This paper deals with testing of MXene nanomaterial properties to be applied for sensor design for measurement of dynamic variables.

With the discovery of many nanomaterials like carbon nanotubes (CNTs), graphene, molybdenum disulfide *etc.*, in the past few decades, the multifunctional nature of these nanomaterials was utilized for developing sensing devices like piezoresistive CNT micro-electro-mechanical sensors,[1] CNT-based actuators,[2] strain sensors[3,4] and pressure sensors.[5] The latest among these two-dimensional (2D) nanomaterials are MXenes (particularly Titanium Carbide, Ti₃C₂; henceforth referred to as Ti₃C₂-MXenes) discovered in 2011.[6,7] Ti₃C₂-MXenes have created a lot of interest for sensor development due to their metallic conductivity (6000–8000 S cm⁻¹),[8,9] capacitance,[10,11] film-forming ability,[12,13] fast response time and good elastic

[a]Academic Center for Materials and Nanotechnology (ACMiN), AGH University of Science and Technology (UST), Krakow, Poland. E-mail: sshreyas@agh.edu.pl; kgrabow@agh.edu.pl

[b]Centre for Nano Science and Engineering (CeNSE), Indian Institute of Science (IISc), Bangalore, India. E-mail: saurabh2203@iisc.ac.in

[c]Atomic, Molecular and Optical Physics Division, Physical Research Laboratory, Ahmedabad, India

[d]Instrumentation and Applied Physics, Indian Institute of Science (IISc), Bangalore, India

† Electronic supplementary information (ESI) available. See DOI: 10.1039/d0ra04879h

properties (*e.g.* Young's modulus $\sim$330 GPa).[14,15] Free-standing films of Ti_3C_2-MXenes have been fabricated and the multifunctional properties of these films have been described including elasticity, electrical conductivity,[14,16,17] electromagnetic interference[18] *etc.* The response of free-standing Ti_3C_2-MXene films have been reported in these literatures using tensile test and nano-indentation tests to quasi-static forces. Even as the physical and chemical properties of Ti_3C_2-MXenes are being explored by many research groups, very few physical sensing capabilities and implementations have been reported in biosensing,[19] strain sensing,[20,21] thermal sensing,[22] piezoresistive pressure sensing,[23,24] flexible strain and chemical sensing[25,26] *etc.* Response of the free-standing Ti_3C_2-MXene films to dynamic changes of repeatable external forces like high-velocity shockwave impact and low-velocity mechanical impact acting on it is not explored. There is a need to consider the dynamic response properties of Ti_3C_2-MXene films when designing sensors for control and health monitoring applications.

This paper focuses on the experimental investigations of free-standing Ti_3C_2-MXene films subjected to dynamic external forces in the form of shockwave and mechanical impact. These tests on the Ti_3C_2-MXene films help study the response of the films to forces which are applied for a very short period of time (μs or ms). The preparation of Ti_3C_2-MXene films, device fabrication, the experimental set-up for testing and the results obtained are all provided in this paper. A shock tube driven by piston and manual mechanical force is used to generate the shockwave and, in another experiment, metallic (stainless steel) balls are used to generate the impact. The response of the Ti_3C_2-MXene films to dynamic forces and their utility in developing sensors are discussed. The response time of the material are reported along with the repeatability test results of the samples.

The choice of the two dynamic forces and the tests through which these forces are applied is selected based on the need for a repeatable source of forcing.[27] Shockwave[28] and impact forces[29] provide repeatable external forces that can be applied to the Ti_3C_2-MXene films for testing. Based on known repeatable input, the response of the Ti_3C_2-MXene films as sensing material has been ascertained. The impact force generated by a ball drop test generates a simple aperiodic forcing function close to a true impulse while the shock tube test generates a step forcing function on the sensing element (sensing element and Ti_3C_2-MXene film sample are used interchangeably throughout the paper). The forces have a time of microseconds and/or milliseconds which causes the Ti_3C_2-MXene film sample to respond in the same time range. The rise time of the Ti_3C_2-MXene response due to the shockwave in the form of changing fluid pressure is very short ($\sim$few μs) while due to mechanical impact is short ($\sim$ms). The limitations of the ball drop test arising from non-precise forcing function (due to the assumptions involved in the test), joint mass effect due to contact between sensing element and ball mass, signal noise and restricted point-concentrated force is overcome by the shock tube test. The incident shockwave or primary shockwave produced in the shock tube creates an approximate uniformly distributed force on the Ti_3C_2-MXene film surface. But this changes when the

shockwave gets reflected within the shock tube. The background for the present investigations are based on the literature works with shock tube test on graphene[28] and impact tests on film structures.[29,30] The shock tube test is conducted using a table-top, manually operated piston driven shock tube comprising of driving and driven section described in literature.[31,32] The ball drop test is performed by dropping the ball from a known height through a glass tube and the Ti_3C_2-MXene film is housed in a support structure similar to these literature works.[29,33–35]

The organization of this paper is given henceforth. The synthesis and device fabrication as a part of Ti_3C_2-MXene film sample preparation is discussed initially. Experimental test set-ups for shock tube test and ball drop test are explained in detail with testing procedures. Then the experimental theory and simple equations used in the process of post-processing is provided. As a follow-up for the synthesis of Ti_3C_2-MXenes, the pure Ti_3C_2-MXene film along with the precursor material (Ti_3AlC_2) are subjected to X-ray diffraction method to confirm the successful synthesis of Ti_3C_2-MXene films. The morphology of the two-dimensional Ti_3C_2-MXene sample is studied under transmission electron microscopy. The Ti_3C_2-MXene film is fabricated into a device for it to be subjected to high-velocity shockwave and low-velocity mechanical impact. The results are analysed and discussed for each test. The indication of piezoresistive behaviour of pure Ti_3C_2-MXene film when subject to both tests are discussed along with conclusions. It is to be noted that this is a first attempt of testing the Ti_3C_2-MXene film samples under the dynamic force conditions of shock and impact and results show repeatable behaviour for the material.

Experimental sample preparation

Ti_3C_2-MXene synthesis and device fabrication

MXenes (Ti_3C_2) are synthesized by *in situ* hydrogen fluoride formation (Lithium Fluoride (LiF) + Hydrogen Chloride (HCl)) using Minimally Intensive Layer Delamination (MILD) method similar to guidelines provided in these literature works.[6,36–38] 2 g amount of Titanium Aluminium Carbide (Ti_3AlC_2; supplier: Carbon-Ukraine Ltd.) is added into etchant solution (6 M HCl and 1.5 g amount of LiF) for 24 h to etch aluminium. Next, the solution is washed until the pH value reaches $\geq$6. The product obtained after washing, is collected and sonicated for 1 h. The resultant black colour solution called Ti_3C_2-MXene are filtered out in vacuum (vacuum-assisted filtration process) to form Titanium Carbide (Ti_3C_2) films.

The Ti_3C_2-MXene films are cut to rectangular strips of millimetre lateral dimensions as mentioned in Table 1. It has been shown in the literature[39] that pure Ti_3C_2-MXene films oxidize if left open in air, become brittle and lose conductivity. To avoid this, samples are laminated (sandwiched) between plastic sheets (thickness: 150 microns per sheet) and stuck on to a support for shock tube and ball drop test. The plastic sheet laminations avoid oxidation as the lamination process provides isolation for the films from external environment (temperature, humidity, dust and damage).[40] Silver epoxy paste is applied at

Table 1 Dimensions of Ti_3C_2-MXene film samples used

Dimension of Ti_3C_2-MXene film sample	Sample 1 (for ball drop test)	Sample 2 (for shock tube test)
Length (mm)	9	12
Width (mm)	2	3
Thickness (µm)	12	12

the Ti_3C_2-MXene sample edges for connection to external instrumentation for output signal processing and recording.

Experimental test set-up

Shock tube test. A simple hand-operated pressure-driven table-top shock tube is the test set-up within which the Ti_3C_2-MXene sample is kept for subjecting it to the shock tube test. The tube is a free piston-driven shock tube. It consists of a driver and driven section. The piston plunger in the driver section is used for compressing the pressurized air (3 bar) stored in this section using an external air supply. The driver section pressure is monitored by a pressure monitor (M/s IRA Ltd., India). A diaphragm made of tracing paper (thickness: 0.08 mm) is used as the separator between the driver and driven section. The driven section contains commercial piezoresistive sensors (NXP Semiconductors USA Inc.) to measure the shock speed as soon as the diaphragm bursts due to compression from the hand-operated piston plunger. The shockwave traveling from one commercial piezoresistive sensor to the other commercial piezoresistive sensor records the voltage variation due to pressure wave propagation. The distance between the two sensors are known and the voltage rise of the two sensors are recorded on the digital storage oscilloscope (Tektronix, TBS 1072B-EDU). The time taken for the shockwave to travel the known distance is provided by the difference in the time of rise of each sensor. This helps in calculating the speed of the shockwave and the Mach number to be noted. All these details are described schematically in Fig. 1 and the specifications of the shock-tube are provided in the ESI S1.† The shockwave travels in supersonic speed with Mach number more than 1.2. The shock tube test set-up can produce shockwaves of speeds varying with Mach number 1.1 to 2.
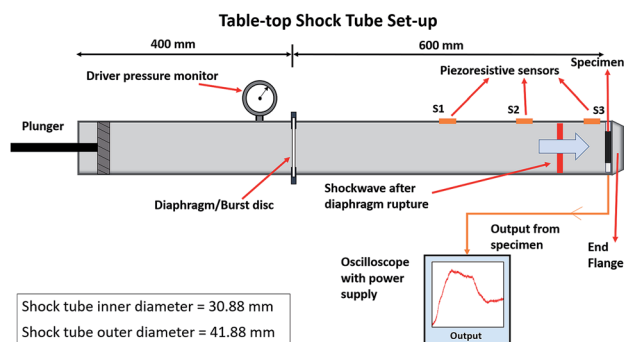
The initial incident or primary shockwave generated due to the diaphragm burst, travels through the driven section and strikes the specimen attached to the end flange. The rupture pressure is in the range of 3–7 bar (ref. 31) which depends on the diaphragm thickness and the force exerted by the person operating the piston plunger and this is measured. Output leads are connected to the Ti_3C_2-MXene film sample. The device fabricated is attached to the glass plate support using a double-sided tape (3 M) and then fixed to the end flange. The device fabricated is illustrated in Fig. 2. The shockwaves travel through the driven section in microseconds and impacts the end flange with Ti_3C_2-MXene film sample before getting reflected inside the driven section. The reflected waves lose energy and dampen out. The double-sided tape used for attaching the glass plate containing Ti_3C_2-MXene film sample dampens the energy due to shockwave impact as well. The primary shockwave impacting the Ti_3C_2-MXene film sample is recorded using the instrumentation set up (signal processing) and this is connected to the digital storage oscilloscope which displays the output. A voltage source (1 V) is provided to the sample through a series resistance (25 Ω) to convert the resistance change into proportional voltage. The variation of resistance due to shockwave impact gets converted to voltage, measuring the instantaneous response. The response is in the time scale of microseconds and the output is recorded. This is illustrated in the Fig. 3.

Ball drop test. The experimental test set-up is designed and developed in-house at CeNSE, IISc. The picture of the test set-up is given in Fig. 4. A glass tube holder with a heavy metal base is the support structure for the glass tube. The glass tubes of particular height can be selected, and this height is typically the drop height of the ball as the metallic ball is dropped from the
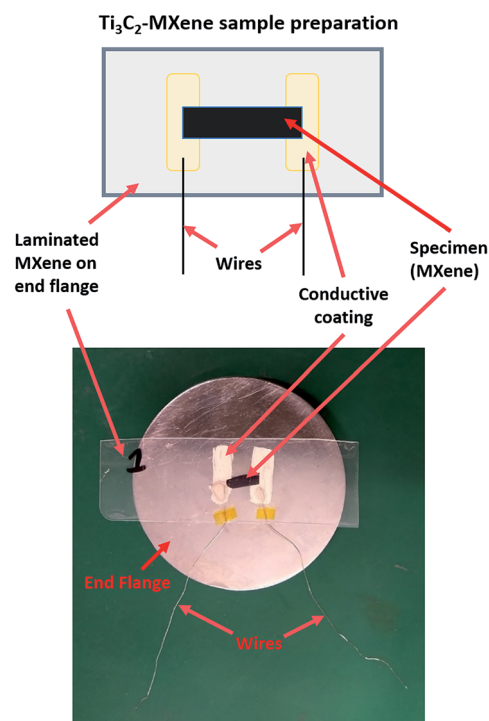

Fig. 1 Experimental test set-up of shock tube with three piezoresistive sensors S1, S2 and S3.

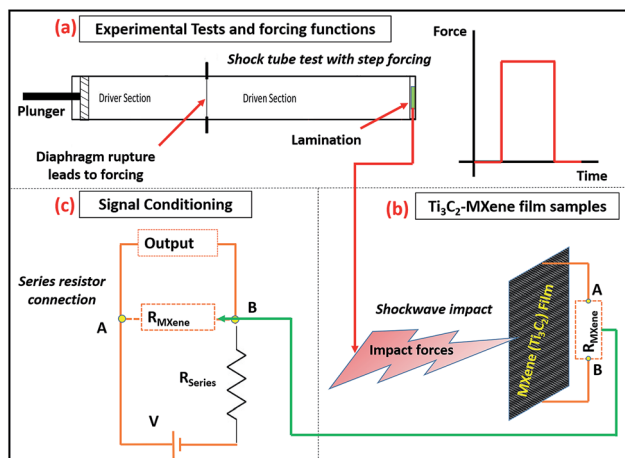
Fig. 2 Experimental sample with lamination and placed on end flange.

Fig. 3 Illustration of the shock tube test on Ti_3C_2-MXene film with signal conditioning to obtain output.

top end of the glass tube while the Ti_3C_2-MXene film is present at the bottom end of the glass tube. The base of the tube holder is made of heavy metal such that the stiffness and mass of the base is very high compared to the ball which is being dropped. This ensures that the natural frequencies of metallic base are much higher than the natural frequencies of the ball and the Ti_3C_2-MXene film sample. Similar method is employed for testing of any metallic component used in mechanical and aerospace systems. The output of the Ti_3C_2-MXene film is recorded through a Wheatstone bridge circuit (average resistance of the other three resistors are 33.68 Ω) and a DC power supply ($V = 1.5$ V; Advanced Electronics System, India) along with digital storage oscilloscope (Gwinstek, GDS-2102A). The diameter of the glass tube and the Ti_3C_2-MXene sample diameter under the tube were approximately the same. The metallic balls made of stainless-steel, fall through the glass tube and have a direct impact on the Ti_3C_2-MXene film (sensing element). The Ti_3C_2-MXene film was held below the glass tube using a holder (polymer support) perpendicular to the tube. The output voltage was recorded for the ball drop with stainless-

steel metallic balls of different diameter and weights. The test set-ups used for the experiment are provided in the table below and Fig. 5 illustrates the experimentation process.

The experiments were repeated for each drop height to achieve better accuracy and repeatability. A concentrated impact force is exerted by the ball when it hits the Ti_3C_2-MXene film at the centre of the Ti_3C_2-MXene film. This results in an impact on the Ti_3C_2-MXene film and the Ti_3C_2-MXene film response is recorded along with the plastic laminations which creates a sandwich with Ti_3C_2-MXene film.

Experimental theory

The theory based on which the calculations for the experiments are carried out for shock tube test and ball drop test are described in this section.

Shock tube test. Shockwaves generated in the shock tube provides a repeatable forcing on the Ti_3C_2-MXene film sample to study its response. In order to calculate the velocity at which the shockwave impacts the Ti_3C_2-MXene film sample, the commercial sensors in the experimental set-up provides the measurement. If d is the distance (mm or 10^{-3} m) between two commercial piezoresistive sensors and t (seconds, s) is the time taken by the shockwave to travel the distance between the two sensors, then the velocity of the shockwave, ϑ_{shock} (ms^{-1}), is given by eqn (1). Mach number (M) is calculated as a ratio of velocity of the shockwave to the velocity of sound in the same medium (air, in the present case) which is given in eqn (2). Here, 'a' is the speed of sound in air (ms^{-1}), γ_1 (=1.4) is the specific heat ratio, R (=287 J kg^{-1}) is specific gas constant and T (=300 K) is the air temperature.

$$\vartheta_{shock} = \frac{d}{t} \tag{1}$$

$$M = \frac{\vartheta_{shock}}{a}; \quad a = (\gamma_1 R T)^{\frac{1}{2}} \tag{2}$$
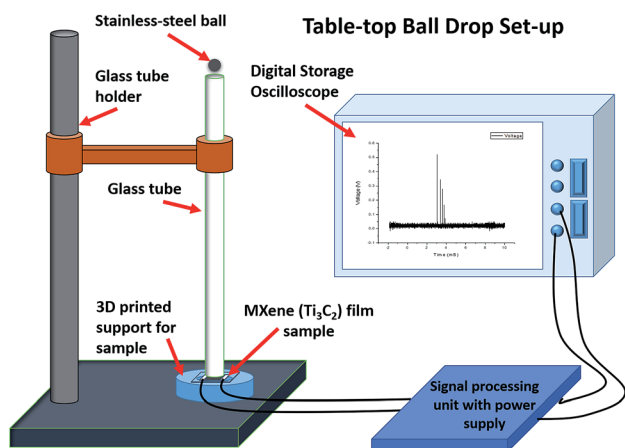

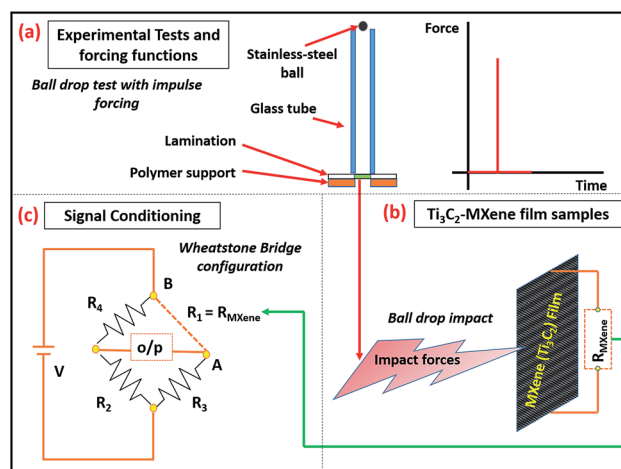**Fig. 4** Illustration of experimental set-up of ball drop test with glass tube and instrumentation.

Fig. 5 Illustration of the ball drop test on Ti_3C_2-MXene film sample with signal conditioning to obtain output.

Ball drop test. The stainless-steel ball of varying diameter and weight is dropped from a fixed height in the experiments conducted in this paper. The effect of parameters of drop height, acceleration due to gravity and mass of the ball on the impact force and velocity of impact is discussed here. The experimental set-up is a specific implementation of the law of conservation of energy. With the assumptions of the air drag in the glass tube and its side walls to be negligible and the acceleration due to gravity to be equal to 9.81 ms^{-2}, the testing condition of the experiment can simplify the energy relationship before and after impact of the ball. The assumptions lead to the deduction that the potential energy before impact is equal to the kinetic energy after impact. Eqn (3) provides the conservation of energy equation, where m is the mass of the of the metallic ball (grams or kg), h is the drop height or length of glass tube (mm or m), g is the acceleration due to gravity (9.81 ms^{-2}), $\vartheta_{\text{impact}}$ (ms^{-1}) is the impact velocity and F_{imp} (N) is the idealized impact force.

$$mgh = \frac{1}{2}m\vartheta_{\text{impact}}^2; \quad F_{\text{imp}} = mg \qquad (3)$$

The eqn (3) also indicates that the impact velocity is independent of the mass and depends on the drop height and acceleration due to gravity resulting in eqn (4).

$$\vartheta_{\text{impact}} = \sqrt{2gh} \qquad (4)$$

Results and discussions

The Ti$_3$C$_2$-MXene films synthesized are characterized to validate the pure MXene film formation. The films are used to fabricate Ti$_3$C$_2$-MXene film sample devices which are subjected to shock tube and ball drop test. All these results are provided in this section and discussion is provided in the respective subsections.

Material characterization of Ti$_3$C$_2$-MXene film

The MXene (Ti$_3$C$_2$) and its parent material (Ti$_3$AlC$_2$) are subjected to XRD (Rigaku Smartlab) to confirm the successful aluminium etching and synthesis of the Ti$_3$C$_2$-MXene (Fig. 6(a)). The characteristic aluminium peak of MAX (Ti$_3$AlC$_2$) phase compound at $\sim$39° completely disappears in MXene (Ti$_3$C$_2$) film.

Additionally, Ti$_3$C$_2$-MXene peak broadens and loses crystallinity due to removal of aluminium. The peak at (002) shifts from 9.5° to 6.7°, indicating the increase in d-spacing (0.9 nm to 1.3 nm). This clearly confirms the successful synthesis of Ti$_3$C$_2$-MXene.[6] Fig. 6(b) shows the two-dimensional sheet like morphology found using Transmission Electron Microscopy (TEM) (Titan Themis 300 kV from FEI), which indicates successful synthesis of Ti$_3$C$_2$-MXene nanosheets. It is observed that Ti$_3$C$_2$-MXene nanosheets are irregular in shape and overlap with each other. The darker region reveals stacking of layers (multilayer) whereas lighter region corresponds to stacking of few layers.
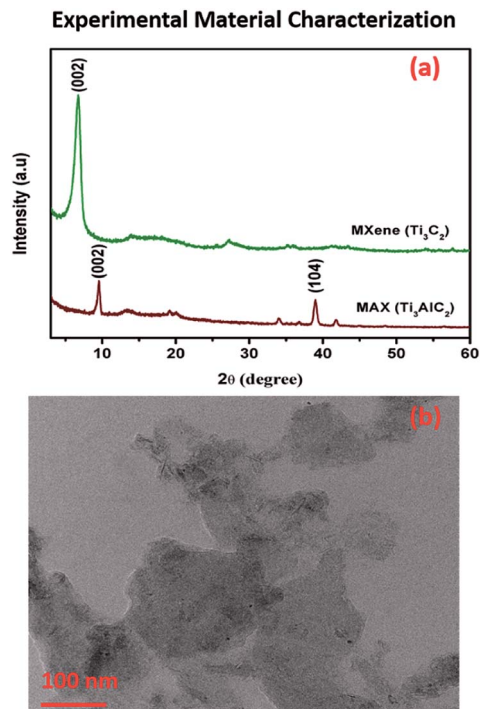

Experimental Material Characterization

Fig. 6 (a) XRD spectra of the MAX (Ti$_3$AlC$_2$) phase and MXene (Ti$_3$C$_2$) compounds (b) TEM image of two-dimensional Ti$_3$C$_2$-MXene nanosheets.

Analysis of shock tube test

The effect of forces due to shockwaves on the Ti$_3$C$_2$-MXene film has been discussed in this section. For the high-velocity shockwave front acting on the Ti$_3$C$_2$-MXene film sample, the response is recorded. The overall experiment time for the shock tube tests conducted is 500 μs. The peak overpressure measured at the end of the tube of driven section is 234.3 kPa or 2.343 bar. The incident pressure acting on the end flange (with diameter of 30 mm) results in a force of about 162.5 N to act on the Ti$_3$C$_2$-MXene film sample mounted on the end flange. The burst of the paper diaphragm results in the shockwave being generated with Mach number of 1.68 (calculation given in ESI S1†). The shockwave generated after diaphragm burst is given in Fig. 7(a) and a particular response of the Ti$_3$C$_2$-MXene film sample is given in Fig. 7(b). The results demonstrate the capability of the Ti$_3$C$_2$-MXene film sample to respond to the external force of shockwave with high-velocity (acting on the sample in time scale of microseconds in the form of a step forcing function). The response time is observed to be 7.13 ± 1.28 μs. The shockwave interaction with the Ti$_3$C$_2$-MXene film sample might cause a dislocation in the nanosheets arrangement of the Ti$_3$C$_2$-MXene film sample which consists of stacked up monolayer Ti$_3$C$_2$-MXenes. Sometimes, this interaction may result in the deviation of the response time. This dislocation leads to change in recorded maximum voltage (in turn resistance) as well as increase in the slope of the response curve (see ESI S1†). A change of the response is observed along with a consistent qualitative behaviour of the Ti$_3$C$_2$-MXene film sample with rise
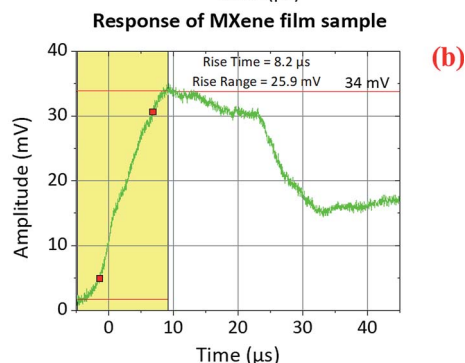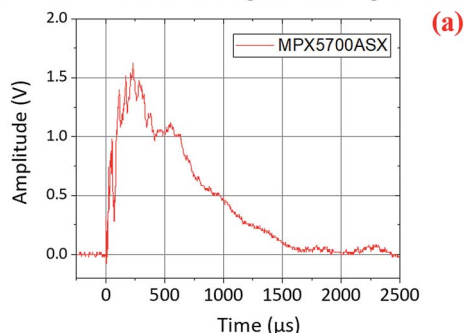
Fig. 7 (a) Measurement of shockwave generated by commercial piezoresistive sensor (b) response of Ti_3C_2-MXene film sample to primary shockwave impact.

and decay of the curve (see ESI S1†) and this qualitative behaviour remains consistent beyond three trials as well. The dislocation might be a result of changes in contact between layers and orientations of monolayer Ti_3C_2-MXene which forms the Ti_3C_2-MXene film. The results of very fast response time for the forcing makes the material a good candidate to develop shockwave measurement sensor while the dislocation behaviour needs more exploration. These microstructural changes need detail study using material characterization methods in future.

Analysis of ball drop test

Ball drop test applies a low-velocity impulse force on the Ti_3C_2-MXene film sample. The forcing depends on the parameters of the stainless-steel balls used for the test. The stainless-steel balls are dropped from a known height for all the trials which are recorded here. The variation in the ball diameter, weight and the tube diameter define the test set-up parameters and is provided in Table 2. The response or rise time is observed to be 1.24 ± 0.43 ms, 1.56 ± 0.03 ms and 1.60 ± 0.01 ms for test set-ups 1, 2 and 3, respectively. The rise time for each test set-up case is provided in detail in ESI S2.† The mean value of response time is observed to increase with the increase in ball weight and diameter. With the increase in the weight of the ball, the impact force exerted on the Ti_3C_2-MXene film sample also increases and this results in longer contact time between the ball and the sample due to higher energy transfer upon impact. This results of increase in response time with impact forces are

Table 2 Physical parameters of ball drop test set-ups used for testing

Physical parameters	Test set up 1	Test set up 2	Test set up 3
Tube height (mm)	300	300	300
Tube diameter (mm)	5	5	12
Ball weight (mg)	131.1	443.2	1049
Ball diameter (mm)	3.14	4.75	6.31
Velocity of impact (m s^{-1})	2.4261	2.4261	2.4261
Impact force (N)	1.2860	4.3477	10.2906
Potential energy (J)	0.3858	1.3043	3.0872

shown in Fig. 8(a) with a sample response for test set-up 3 shown in Fig. 8(b).

Distinct voltage output for each weight and diameter of the stainless-steel ball provides an evidence of particular response of the Ti_3C_2-MXene film sample for individual input force (see ESI S2†). In the present experiment, the density of the ball is kept constant (stainless-steel) and the variation of weight and diameter is captured with varying response of Ti_3C_2-MXene. The test results provide enough evidence to develop an impact sensor for non-destructive material characterization.

Comparison of results and piezoresistive behaviour

The results from shock tube test and ball drop test characterizes the dynamic response time (an important sensing element material property) of the pure Ti_3C_2-MXene film material to be in range of microseconds and milliseconds, respectively. These responses are for different forcing functions acting with
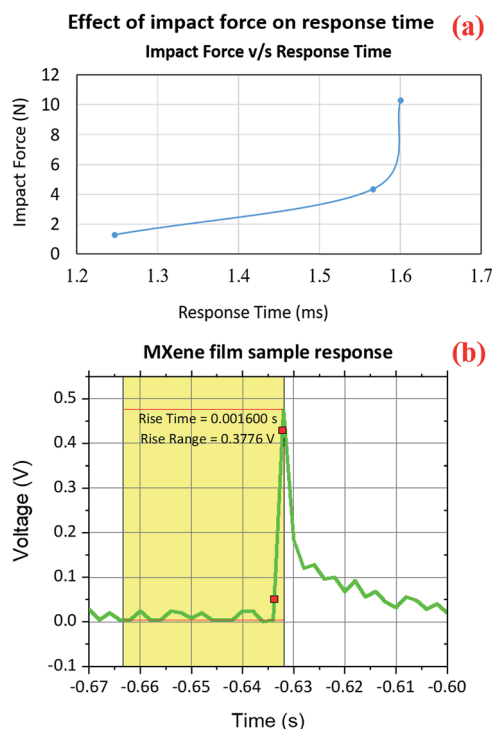

Fig. 8 (a) Variation of response time due to impact forces with changing ball weight (b) response of Ti_3C_2-MXene film sample for ball drop impact (test set-up 3).

different time scales. The results also indicate that with either shockwave impact created by fluid medium or mechanical impact created by a solid causes deformation in the Ti_3C_2-MXene film sample (in turn Ti_3C_2-MXene monolayer stacking). The changes in resistance measured is converted to voltage output and recorded. The effect of change in resistance due to applied forces indicate piezoresistive behaviour of the sensing element material.[41] This proves the observation made in literature about piezoresistive behaviour for Ti_3C_2-MXene based sensor[24] (where nano-indentation test was conducted to demonstrate piezoresistive behaviour). Fig. 9(a) indicates the change in voltage response recorded by repeated impact of shock on the same Ti_3C_2-MXene film sample. The peak output voltage increases with each impact. Thus, indicating a microstructural change due to loading, leading to deformation in the material causing resistance change. Similarly, Fig. 9(b) captures the response of the Ti_3C_2-MXene film sample to ball drop test. The ball which drops from a certain height applies force on the Ti_3C_2-MXene film sample and the response is captured as resistance change (converted to voltage output). The ball after initial impact bounces multiple times as all the kinetic energy is not transferred to the Ti_3C_2-MXene film upon first impact. These multiple bounces of the ball have reducing forces and energy with each successive bounce. The Ti_3C_2-MXene film sample undergoes deformation and because of restitution it gets back to original shape. This causes changes in resistance as well. The literature work[23,24] modify the Ti_3C_2-MXene material and use it as sensor device and demonstrate piezoresistive

behaviour for quasi-static forces. But with the present work we find that the pure Ti_3C_2-MXene films inherently (laminated with plastic sheets to avoid faster oxidation behaviour and loss of conductivity) have significant piezoresistive behaviour which can be utilized for sensor design and development. In the present work the dynamic response time is about ~7 μs for forces from shockwave and ~1.5 ms (average) for forces from mechanical impact. These response times are significantly better than the ones reported in literature, namely, 30 ms,[24] 88 ms [42] and 138 ms [23] (detail comparison with commercial sensors are also provided in the ESI S3†). This also signifies the need for good sensor packaging and signal conditioning with a good sensing element (with fast response time). These results and discussions provide a plethora of opportunities for sensor design for various dynamic phenomena leading to better control and health monitoring of mechanical and aerospace systems along with biomedical devices.

Conclusions

The dynamic response properties of the Ti_3C_2-MXene film sample have been studied for the first time for both low-velocity mechanical impact force (ball drop test) and high-velocity shockwave force (shock tube test). The Ti_3C_2-MXene material is found to respond well for both velocity ranges indicating its use for sensing elements during sensor design for measurement of dynamic phenomena. The shockwave interaction with Ti_3C_2-MXene film results in a response time of 7.13 ± 1.28 μs. The deviation of the results indicates a dislocation in the Ti_3C_2-MXene stack assembly (which forms the Ti_3C_2-MXene film sample) due to shockwave interaction. The very fast response time of the Ti_3C_2-MXene film samples provides the basis for development of shockwave measurement sensor. For the ball drop test conducted, the response time for three different test set-ups (with increasing stainless-steel ball diameter and weight) are 1.24 ± 0.43 ms, 1.56 ± 0.03 ms and 1.60 ± 0.01 ms, respectively. The contact time between the ball and Ti_3C_2-MXene film sample increases with increasing weight and thus results in increasing response time. The distinct voltage output got for each stainless-steel ball provides a basis for using the Ti_3C_2-MXene film sample as impact sensor. The variation of resistance of the pure Ti_3C_2-MXene film sample to dynamic forces is converted to voltage output through signal processing. The response from both high-velocity shockwave impact and low-velocity mechanical impact indicate significant piezoresistive behaviour. The results indicate that the Ti_3C_2-MXene nanomaterial-based film has inherent piezoresistivity. The paper presents the evidence of fast response time of Ti_3C_2-MXene film sample (~1.5 ms and ~7 μs) compared to published literature works. Finally, the response time measurement is an important quantitative parameter that forms the basis of sensor design for measurement of dynamically varying parameters of pressure, force, accelerations *etc.*

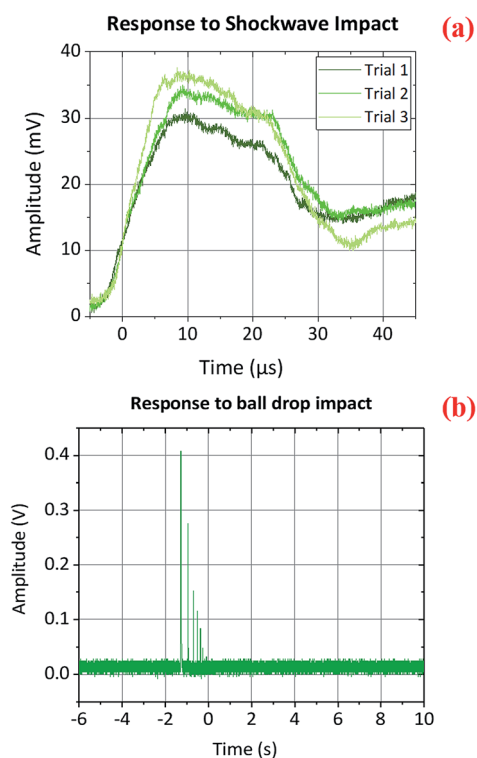## Conflicts of interest

There are no conflicts to declare.

Fig. 9 (a) Response of Ti_3C_2-MXene film sample to multiple impacts of shockwave (b) full spectrum response of Ti_3C_2-MXene film sample for ball drop impacts (test set-up 3).

Acknowledgements

References

1 M. A. Cullinan and M. L. Culpepper, Carbon nanotubes as piezoresistive microelectromechanical sensors: theory and experiment, *Phys. Rev. B: Condens. Matter Mater. Phys.*, 2010, **82**(11), 1–6, DOI: 10.1103/PhysRevB.82.115428.

2 C. Li, E. T. Thostenson and T. W. Chou, Sensors and actuators based on carbon nanotubes and their composites: a review, *Compos. Sci. Technol.*, 2008, **68**(6), 1227–1249, DOI: 10.1016/j.compscitech.2008.01.006.

3 K. Grabowski, *Design and Development of the Sensors for Structural Health Monitoring (SHM) based on the Carbon Nanomaterials*, AGH University of Science and Technology, 2017.

4 G. Yin, N. Hu, Y. Karube, Y. Liu, Y. Li and H. Fukunaga, A carbon nanotube/polymer strain sensor with linear and anti-symmetric piezoresistivity, *J. Compos. Mater.*, 2011, **45**(12), 1315–1323, DOI: 10.1177/0021998310393296.

5 M. S. Manjunath, N. Nagarjuna, G. Uma, M. Umapathy, M. M. Nayak and K. Rajanna, Design, fabrication and testing of reduced graphene oxide strain gauge based pressure sensor with increased sensitivity, *Microsyst. Technol.*, 2018, **24**(7), 2969–2981, DOI: 10.1007/s00542-018-3782-9.

6 M. Naguib, M. Kurtoglu, V. Presser, J. Lu, J. Niu, M. Heon, L. Hultman, Y. Gogotsi and M. W. Barsoum, Two-Dimensional Nanocrystals Produced by Exfoliation of Ti_3AlC_2, *Adv. Mater.*, 2011, **23**(37), 4248–4253, DOI: 10.1002/adma.201102306.

7 X. Zhan, C. Si, J. Zhou and Z. Sun, MXene and MXene-based composites: synthesis, properties and environment-related applications, *Nanoscale Horiz.*, 2020, **5**(2), 235–258, DOI: 10.1039/C9NH00571D.

8 F. Shahzad, M. Alhabeb, C. B. Hatter, B. Anasori, S. M. Hong, C. M. Koo and Y. Gogotsi, Electromagnetic interference shielding with 2D transition metal carbides (MXenes), *Science*, 2016, **353**(6304), 1137–1140, DOI: 10.1126/science.aag2421.

9 Y. Yu, J. Zhou and Z. Sun, Modulation engineering of 2D MXene-based compounds for metal-ion batteries, *Nanoscale*, 2019, **11**(48), 23092–23104, DOI: 10.1039/C9NR08217D.

10 M. Hu, R. Cheng, Z. Li, T. Hu, H. Zhang, C. Shi, J. Yang, C. Cui, C. Zhang, H. Wang, B. Fan, X. Wang and Q. H. Yang, Interlayer engineering of $Ti_3C_2T_x$ MXenes towards high capacitance supercapacitors, *Nanoscale*, 2020, **12**(2), 763–771, DOI: 10.1039/C9NR08960H.

11 M. Cao, F. Wang, L. Wang, W. Wu, W. Lv and J. Zhu, Room Temperature Oxidation of Ti_3C_2 MXene for Supercapacitor Electrodes, *J. Electrochem. Soc.*, 2017, **164**(14), A3933–A3942, DOI: 10.1149/2.1541714jes.

12 Z. Ling, C. E. Ren, M.-Q. Zhao, J. Yang, J. M. Giammarco, J. Qiu, M. W. Barsoum and Y. Gogotsi, Flexible and conductive MXene films and nanocomposites with high capacitance, *Proc. Natl. Acad. Sci. U. S. A.*, 2014, **111**(47), 16676–16681, DOI: 10.1073/pnas.1414215111.

13 Z. Fu, N. Wang, D. Legut, C. Si, Q. Zhang, S. Du, T. C. Germann, J. S. Francisco and R. Zhang, Rational Design of Flexible Two-Dimensional MXenes with Multiple Functionalities, *Chem. Rev.*, 2019, **119**(23), 11980–12031, DOI: 10.1021/acs.chemrev.9b00348.

14 A. Lipatov, H. Lu, M. Alhabeb, B. Anasori, A. Gruverman, Y. Gogotsi and A. Sinitskii, *Sci. Adv.*, 2018, **4**(6), 1–8.

15 J. L. Hart, K. Hantanasirisakul, A. C. Lang, B. Anasori, D. Pinto, Y. Pivak, J. T. van Omme, S. J. May, Y. Gogotsi and M. L. Taheri, Control of MXenes' electronic properties through termination and intercalation, *Nat. Commun.*, 2019, **10**(1), 522, DOI: 10.1038/s41467-018-08169-8.

16 J. Lipton, G.-M. Weng, M. Alhabeb, K. Maleski, F. Antonio, J. Kong, Y. Gogotsi and A. Taylor, Mechanically strong and electrically conductive multilayer MXene nanocomposites, *Nanoscale*, 2019, **11**(42), 20295–20300, DOI: 10.1039/c9nr06015d.

17 B. Anasori, C. Shi, E. J. Moon, Y. Xie, C. A. Voigt, P. R. C. Kent, S. J. May, S. J. L. Billinge, M. W. Barsoum and Y. Gogotsi, Control of electronic properties of 2D carbides (MXenes) by manipulating their transition metal layers, *Nanoscale Horiz.*, 2016, **1**(3), 227–234, DOI: 10.1039/C5NH00125K.

18 L. Wang, L. Chen, P. Song, C. Liang, Y. Lu, H. Qiu, Y. Zhang and J. Kong, 3D $Ti_3C_2T_x$ MXene/C hybrid foam/epoxy nanocomposites with superior electromagnetic interference shielding performances and robust mechanical properties, *Composites, Part B*, 2019, **171**(5), 111–118, DOI: 10.1016/j.compositesa.2019.05.030.

19 A. Sinha, H. Z. Dhanjai, Y. Huang, X. Lu, J. Chen and R. Jain, MXene: an emerging material for sensing and biosensing, *TrAC, Trends Anal. Chem.*, 2018, **105**, 424–435, DOI: 10.1016/j.trac.2018.05.021.

20 Y. Yang, L. Shi, Z. Cao, R. Wang and J. Sun, Strain Sensors with a High Sensitivity and a Wide Sensing Range Based on a $Ti_3C_2T_x$ (MXene) Nanoparticle–Nanosheet Hybrid Network, *Adv. Funct. Mater.*, 2019, **29**(14), 1–10, DOI: 10.1002/adfm.201807882.

21 K. Yang, F. Yin, D. Xia, H. Peng, J. Yang and W. Yuan, A highly flexible and multifunctional strain sensor based on a network-structured MXene/polyurethane mat with ultra-high sensitivity and a broad sensing range, *Nanoscale*, 2019, **11**(20), 9949–9957, DOI: 10.1039/C9NR00488B.

22 T. H. Park, S. Yu, M. Koo, H. Kim, E. H. Kim, J. E. Park, B. Ok, B. Kim, S. H. Noh, C. Park, E. Kim, C. M. Koo and C. Park, Shape-Adaptable 2D Titanium Carbide (MXene) Heater,

ACS Nano, 2019, **13**(6), 6835–6844, DOI: 10.1021/acsnano.9b01602.

23 Y. Yue, N. Liu, W. Liu, M. Li, Y. Ma, C. Luo, S. Wang, J. Rao, X. Hu, J. Su, Z. Zhang, Q. Huang and Y. Gao, 3D hybrid porous Mxene-sponge network and its application in piezoresistive sensor, *Nano Energy*, 2018, **50**, 79–87, DOI: 10.1016/j.nanoen.2018.05.020.

24 Y. Ma, N. Liu, L. Li, X. Hu, Z. Zou, J. Wang, S. Luo and Y. Gao, A highly flexible and sensitive piezoresistive sensor based on MXene with greatly changed interlayer distances, *Nat. Commun.*, 2017, **8**(1), 1207, DOI: 10.1038/s41467-017-01136-9.

25 L. Zhao, K. Wang, W. Wei, L. Wang and W. Han, High-performance flexible sensing devices based on polyaniline/MXene nanocomposites, *InfoMat*, 2019, **1**(3), 407–416, DOI: 10.1002/inf2.12032.

26 X. Shi, H. Wang, X. Xie, Q. Xue, J. Zhang, S. Kang, C. Wang, J. Liang and Y. Chen, Bioinspired Ultrasensitive and Stretchable MXene-Based Strain Sensor via Nacre-Mimetic Microscale "Brick-and-Mortar" Architecture, *ACS Nano*, 2019, **13**(1), 649–659, DOI: 10.1021/acsnano.8b07805.

27 J. L. Schweppe, *Methods for the Dynamic Calibration of Pressure Transducers*, Department of Commerce National Bureau of Standards, US Deptartment of Commerce, Washington D.C., 1963.

28 S. L. Chinke, I. S. Sandhu, D. R. Saroha and P. S. Alegaonkar, Graphene-Like Nanoflakes for Shock Absorption Applications, *ACS Appl. Nano Mater.*, 2018, **1**(11), 6027–6037, DOI: 10.1021/acsanm.8b01061.

29 S. Joshi, G. M. Hegde, M. M. Nayak and K. Rajanna, A novel piezoelectric thin film impact sensor: Application in non-destructive material discrimination, *Sens. Actuators, A*, 2013, **199**, 272–282, DOI: 10.1016/j.sna.2013.06.010.

30 *28th International Symposium on Shock Waves*, ed. K. Kontis, Springer Berlin Heidelberg, Berlin, Heidelberg, 2012.

31 K. P. J. Reddy and N. Sharath, Manually operated piston-driven shock tube, *Curr. Sci.*, 2013, **104**(2), 172–176.

32 G. Jagadeesh, Fascinating world of shock waves, *Resonance*, 2008, **13**(8), 752–767, DOI: 10.1007/s12045-008-0082-1.

33 J. Park, S. Ha and F.-K. Chang, Monitoring Impact Events Using a System-Identification Method, *AIAA J.*, 2009, **47**(9), 2011–2021, DOI: 10.2514/1.34895.

34 Y. Fujii and J. D. R. Valera, Impact force measurement using an inertial mass and a digitizer, *Meas. Sci. Technol.*, 2006, **17**(4), 863–868, DOI: 10.1088/0957-0233/17/4/035.

35 B. P. Chandra, V. K. Chandra, S. K. Mahobia, P. Jha, R. Tiwari and B. Haldar, Real-time mechanoluminescence sensing of the amplitude and duration of impact stress, *Sens. Actuators, A*, 2012, **173**(1), 9–16, DOI: 10.1016/j.sna.2011.09.043.

36 A. Lipatov, M. Alhabeb, M. R. Lukatskaya, A. Boson, Y. Gogotsi and A. Sinitskii, Effect of Synthesis on Quality, Electronic Properties and Environmental Stability of Individual Monolayer Ti_3C_2 MXene Flakes, *Adv. Electron. Mater.*, 2016, **2**(12), 1600255, DOI: 10.1002/aelm.201600255.

37 M. Alhabeb, K. Maleski, B. Anasori, P. Lelyukh, L. Clark, S. Sin and Y. Gogotsi, Guidelines for Synthesis and Processing of Two-Dimensional Titanium Carbide ($Ti_3C_2T_x$ MXene), *Chem. Mater.*, 2017, **29**(18), 7633–7644, DOI: 10.1021/acs.chemmater.7b02847.

38 X. Sang, Y. Xie, M. W. Lin, M. Alhabeb, K. L. Van Aken, Y. Gogotsi, P. R. C. Kent, K. Xiao and R. R. Unocic, Atomic Defects in Monolayer Titanium Carbide ($Ti_3C_2T_x$) MXene, *ACS Nano*, 2016, **10**(10), 9193–9200, DOI: 10.1021/acsnano.6b05240.

39 T. Habib, X. Zhao, S. A. Shah, Y. Chen, W. Sun, H. An, J. L. Lutkenhaus, M. Radovic and M. J. Green, Oxidation stability of $Ti_3C_2T_x$ MXene nanosheets in solvents and composite films, *npj 2D Mater. Appl.*, 2019, **3**(1), 1–6, DOI: 10.1038/s41699-019-0089-3.

40 D. C. Berridge and S. P. Schneider, Calibration of PCB-132 Sensors in a Shock Tube, in *Rto-Avt-200-25*, 2012, pp. 1-14.

41 A. S. Fiorillo, C. D. Critello and A. S. Pullano, Theory, technology and applications of piezoresistive sensors: a review, *Sens. Actuators, A*, 2018, **281**, 156–175, DOI: 10.1016/j.sna.2018.07.006.

42 V. Kedambaimoole, N. Kumar, V. Shirhatti, S. Nuthalapati, P. Sen, M. M. Nayak, K. Rajanna and S. Kumar, Laser-Induced Direct Patterning of Free-standing Ti_3C_2 –MXene Films for Skin Conformal Tattoo Sensors, *ACS Sens.*, 2020, **5**(7), 2086–2095, DOI: 10.1021/acssensors.0c00647.